

We are IntechOpen, the world's leading publisher of Open Access books Built by scientists, for scientists

4,800

Open access books available

122,000

International authors and editors

135M

Downloads

Our authors are among the

154

Countries delivered to

TOP 1%

most cited scientists

12.2%

Contributors from top 500 universities



WEB OF SCIENCE™

Selection of our books indexed in the Book Citation Index
in Web of Science™ Core Collection (BKCI)

Interested in publishing with us?
Contact book.department@intechopen.com

Numbers displayed above are based on latest data collected.
For more information visit www.intechopen.com



The Kidney

Ercan Ayaz

Abstract

Ultrasound and conventional radiographs still remain the first-line radiological tools for most of the kidney disorders. Ultrasonographic image quality has been astonishingly improved in recent years with the development of technology and software algorithms. In line with these developments, ultrasound is not only the primary imaging modality for kidney anatomy and lesions, but also sufficient for definitive diagnosis and follow up for some lesions. The aim of this chapter is to focus on the areas that ultrasound is used primarily about the kidney. These topics include kidney anatomy, anatomic variants that mimic lesions, congenital diseases, kidney stones, nephrocalcinosis, most of the cystic diseases, and some solid lesions, infection, and trauma.

Keywords: kidney, ultrasound, renal cyst, kidney stone, nephrocalcinosis

1. Introduction

Major functions of the kidney are excreting metabolic waste products and maintaining homeostasis by regulating water, salt, and acid-base balance. The kidney is also an endocrine organ that secretes many hormones, including erythropoietin, renin, and prostaglandins. Ultrasound (US) represents the first-line radiologic imaging technique in the assessment of the kidney anatomy and various disorders. Imaging quality of US has greatly developed in recent years with the advances in the transducer, beam-former technology, and image processing software. Grayscale B-mode US, with the addition of tissue harmonic imaging and compound modes, and color Doppler US definitely provide a diagnostic clue in most renal abnormalities. US artifacts are extremely important in the US evaluation of the kidney because they must be differentiated by true images and may add valuable information in some lesions such as stone and cyst. US presents several advantages over the other imaging modalities including low financial cost, portability, availability, lack of restrictions in performing frequent serial examinations at short intervals, and absence of exposure to radiation or nuclear tracers.

In this chapter, grayscale US findings of normal kidney anatomy, anatomic variants, congenital anomalies, kidney stones, cystic and solid lesions, infections, and traumatic lesions have been discussed. Moreover, embryology and anatomy of the kidney have been explained along with the sonography technique briefly.

2. Embryology and anatomy

During the third week of the development of the human embryo, the urogenital apparatus derives from the intermediate mesoderm. The intermediate mesoderm

initially divides into a set of small cell groups called nephrotomes in the cervical and thoracolumbar regions. These cell masses represent three different excretory sets: the pronephros, the mesonephros, and the metanephros. The pronephros is formed at the beginning of the fourth week and remains rudimentary. It is analogous to the kidney in primitive fishes. The mesonephros appears at the end of the fourth week and it is the first functioning unit until the development of metanephros at the ninth week [1]. It is analogous to the kidney of amphibians. Metanephros begins to be active in the 9–10th week [45]. After that time, it becomes a permanent kidney. Metanephros divided into two parts, which originate from different sources, called the metanephric mass and the metanephric diverticulum. The metanephric mass derived from intermediate mesoderm and their cells give rise to nephrons which are the morphological functional units of the kidney. The metanephric diverticulum or ureteric bud develops from mesonephric duct, which constitutes collecting tubules, calices, renal pelvis, and ureter.

Initially, the permanent kidneys are located close to each other in the pelvis at the caudal end of the mesonephros and ventrally to the sacrum. With fetal growth, the kidneys progressively come to the retroperitoneum and move farther apart, while the abdomen and pelvis grow. At the end of the eighth week, the kidneys set themselves at the first four lumbar vertebral levels, just below the adrenal glands. This migration occurs not only by the caudal migration of the kidneys, but also the growth of the caudal part of the body away from the kidneys. The hilum of the kidney, which includes renal pelvis, vessels, and nerves, faces ventrally before migration; it rotates medially almost 90° during the ascent of kidney. In the ninth week, the renal pelvis is directed anteromedially [1].

During fetal life, the human kidney surface is lobulated which decreases gradually at the end of pregnancy but is still present in the kidneys of neonates. Lobulation disappears during infancy. The reason of the lobulation is the caliceal structure of the collecting system [45]. The buds of minor calices penetrate into the metanephric blastema and give rise to 13 trees of excretory ductules. Every minor calyx brings on a big glandular unit that consists of a medullar unit called Malpighi pyramid and a cortical unit which is separated from the others by interlobular sulci that causes lobulated surface of the kidney. Metanephric tissue penetrates between the pyramids, goes toward renal pelvis, and constitutes the Bertin column [1].

Primarily, fetal kidney derives blood supply, branches from the iliac artery. As the kidney ascends, it receives new branches from the abdominal aorta. Meanwhile, the branches from iliac artery undergo involution and disappear. Migration of the kidney ends at the ninth week, when the kidney takes tight contact with the suprarenal gland. Finally, the kidney receives the permanent renal arteries originating from the abdominal aorta. About 70% of people exhibit single renal artery to each kidney. On the other hand, two to four renal arteries are seen in 25% of adults [2]. The supernumerary arteries usually originate from the abdominal aorta above or below the main renal artery and follow it through the renal hilum. However, they may also enter the kidney from the superior and/or the inferior pole which is called polar artery. Inferior polar artery may cross anterior the ureter and occlude it, leading to hydronephrosis. It is important to recognize supernumerary arteries, since if an accessory artery is damaged or ligated, the region of the kidney supplied by it may undergo ischemia.

In the adult, each kidney is located in the retroperitoneum and measures approximately 10–12 cm long, 2–3 cm thick, and 3–5 cm wide and weighs 250–270 g [3]. The right kidney is located posterior to the inferior surface of the liver with peritoneal interposition, and lateral to the second portion of the duodenum without any peritoneal interposition since the second portion of the duodenum is retroperitoneal. The left kidney lies posterior to the pancreatic tail, the stomach, the ligament of Treitz, and posterior medial to the spleen.

The volume of the right kidney is smaller than that of the left kidney, possibly due to limited potential space for the right kidney (large volume of liver in the right upper quadrant) or relatively increased left renal flow (left kidney is closer to aorta and left renal artery is shorter than right renal artery) [4].

The kidney is a bean shaped organ with a smooth, regular border. Renal hilum is located at the medial surface of the kidney and continues with a central cavity called renal sinus. Renal sinus contains the major branches of the renal artery, major tributaries of the renal vein, and the collecting system [5]. The background of renal pelvis is composed of fat tissue. Renal pelvis is generally located posterior to the vessels. The kidney is covered by a renal capsule which is composed of an inner fibrous layer and an outer perinephric adipose layer. Renal cortex is the outer part of the kidney between fibrous renal capsule and the renal medulla. It has a smooth outer contour with a number of projections (columns of Bertin) extending between the Malpighi pyramids. Renal medulla is the inner part of the kidney consisting of a number of 8–18 cone shaped sections, known as renal pyramids. The inner tip of each renal pyramid is called renal papilla where the urine drains into the renal pelvis. The renal pelvis extrudes from the kidney anteromedially and continues as the ureter. The left kidney is usually located 1–2 cm higher than the right kidney and in supine position; right renal pelvis is usually located at the level of the second lumbar vertebra [6].

Renal pyramids are hypoechoic relative to the cortex in the adult kidney which allows demonstrating both structures in ultrasound. The renal cortex should be hypo- or isoechoic relative to the adjacent liver or spleen in most of the normal adults. Hyperechoic renal cortex showed a specificity of 96% and a positive predictive value of 67% for detecting abnormal renal function, but with a poor sensitivity (20%) [7]. However, in neonates, renal cortex is iso- or hyperechoic relative to liver and spleen parenchyma and pyramids are more prominent. Even in premature infants, cortical hyperechogenicity is more prominent [8]. However, an excessive increased renal echogenicity in newborns may also be due to infantile polycystic kidney disease, hemolytic-uremic syndrome, or renal vein thrombosis [8]. Within the range of 2–6 months, the kidneys become gradually less echogenic than the liver and assume the features of the adult kidney between 6 and 24 months of life [3].

There are some variations that affect the border and cortex of the kidney such as junctional parenchymal defect, fetal lobulations, dromedary hump, and hypertrophied column of Bertin (HCB) (**Figure 1**). HCB is an unresorbed polar parenchyma from one or both of the two subdivisions of kidneys that combine to form the normal kidney [9]. HCB is generally located at the junction of the upper and middle thirds of the kidney and contain renal cortex which extends to the renal sinus. HCB also contains adjacent renal pyramids and usually measures less than 3 cm [10]. Sometimes, echogenicity of the HCBs is different from the adjacent renal cortex due to alterations in tissue orientation, which result in different acoustic reflectivity [9]. It may be challenging to differentiate a small, avascular tumor from an HCB, and occasionally contrast enhanced computed tomography (CT) may be necessary to differentiate them.

Junctional parenchymal defects occur at the site of two parenchymal masses called ranunculi which constitute the normal kidney. It is a horizontally oriented linear echogenicity most often located anterior and superiorly and traced medially into the renal sinus.

Dromedary hump is a prominent bulging on the superolateral aspect of the left kidney. It is believed to arise secondary to compression of the upper pole of the left kidney by the spleen during development. The normal nature of this finding is appreciated by the constant thickness of the bulging renal cortex over the underlying renal calyces.

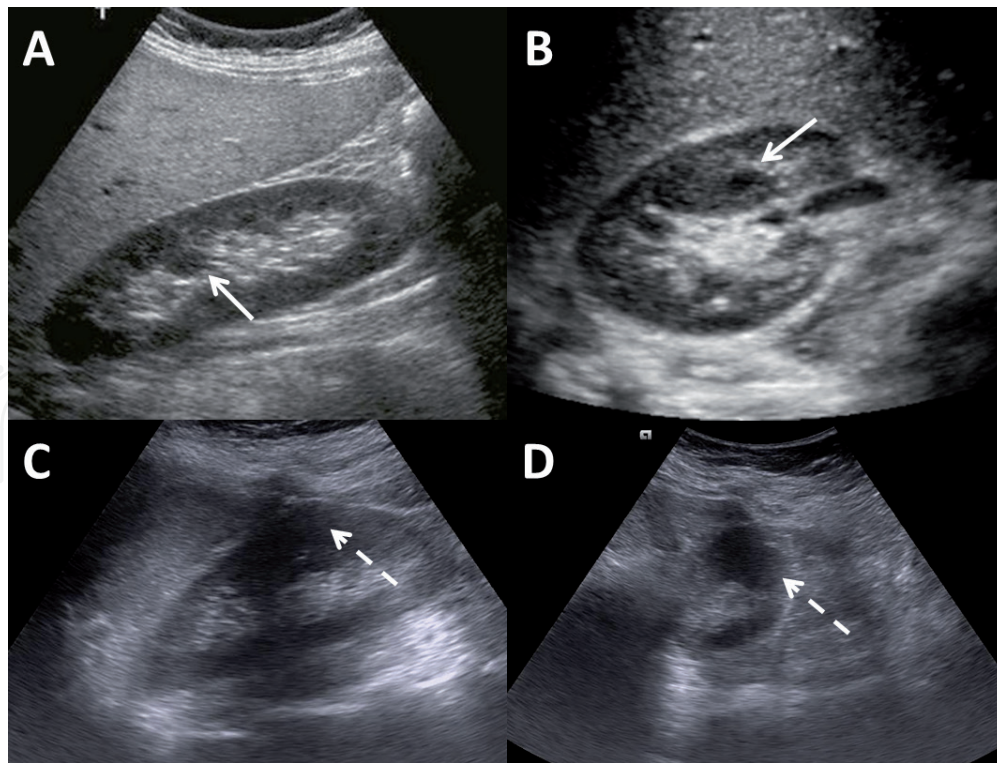


Figure 1. Congenital variations of the kidney. On sagittal (A) and transverse (B) section of the kidney, hypertrophied column of Bertini (arrow) is seen as a hypoechoic cortical extension to the renal sinus. Sagittal (C) and transverse (D) section of another kidney reveals cortical bulging (dashed arrow) on the superolateral aspect, adjacent to the spleen termed as “dromedary hump”.

3. Sonography technique

Before the examination, the adult patients should fast for a minimum of 6 hours before the examination to avoid extensive bowel gas. Convex-array US transducers (with a frequency of 2–5 MHz in adults and 5–8 MHz in pediatric patients) are usually preferred for the US scanning of the kidney. In newborns and infants, even in children, liner US transducers with higher frequency (8–12 MHz) should be additionally employed for better evaluation of cortex and medulla. Tissue harmonic imaging and compound imaging may often be useful for increasing lesion conspicuity and decreasing artifacts [11].

Optimal patient positioning depends on patient habitus, but supine and lateral decubitus positions are often sufficient; while the breath-hold technique is frequently necessary to obtain a complete examination of the renal parenchyma. If there is bowel gas superposition on subcostal view, intercostal window can be used to display kidneys on both sides. The kidneys should be evaluated in the transverse and coronal plane from the superior tip to the inferior [11].

4. Congenital anomalies

Ectopic kidneys are generally located at the pelvis (**Figure 2B**); however, it can be rarely located in the thorax. Crossed renal ectopia is defined as the presence of both kidneys in the same side of the body. The ectopic kidney is fused to the normal kidney in 85–90% of cases called crossed fused ectopy [12]. The upper pole of the ectopic kidney is commonly fused to the lower pole of the normal kidney. Fusion of the kidneys limits the ascent while developments, and thus, both kidneys are located caudally.

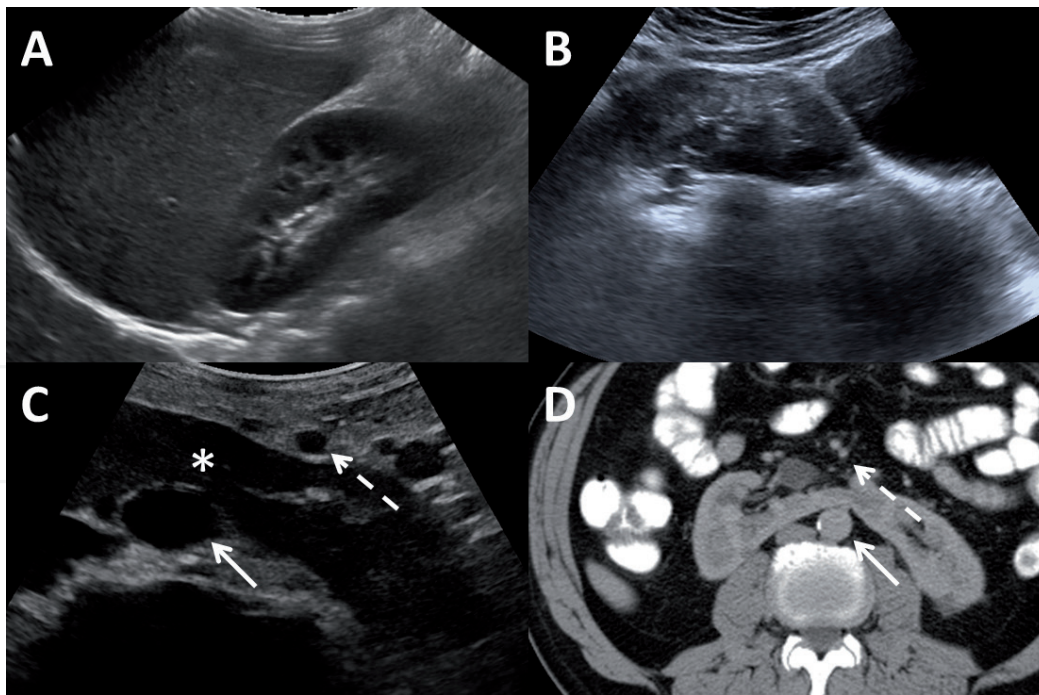


Figure 2.
Congenital anomalies of the kidney. Normal kidney is located inferomedially adjacent to the liver (A). An example of a right ectopic kidney located adjacent to the bladder (B). Ultrasound (C) and computed tomography (D) image of a horseshoe kidney reveals that right and left kidney fused from lower poles at the midline (asterix) from lower poles (asterix) and located between abdominal aorta (arrow) and inferior mesenteric artery (dashed arrow).

Horseshoe kidney is the fusion of the both metanephrogenic blastema from the lower poles prior to migration cranially. Isthmus may compose of either functioning renal cortex or fibrous tissue. The horseshoe kidney is more prone to infection and stone formation due to abnormal rotation of renal pelvis and ureteropelvic junction obstruction. On ultrasound, the horseshoe kidney is located more caudal than usual location and lower poles project inferomedially. Renal isthmus can be seen in the lower abdomen crossing the midline anterior to the aorta (**Figure 2C,D**).

Ureteropelvic junction (UPJ) obstruction is a common anomaly with a male preponderance and the left kidney suffers twice as frequently as the right kidney [13]. Patients with UPJ obstruction have an increased incidence of multicystic dysplastic kidney and renal agenesis of the other kidney. On ultrasound, marked hydronephrosis is present proximal to the level of UPJ obstruction along with normal caliber of the ureter. If long standing, renal parenchymal atrophy accompanies severe dilatation of the renal pelvis.

5. Nephrolithiasis and nephrocalcinosis

Nephrolithiasis is termed as calcification within the collecting system, bladder, ureter, and calyceal system, while nephrocalcinosis is defined as the deposition of calcium salts in the renal parenchyma.

Nephrolithiasis is a common disease with a prevalence of 2–3% in general population and 1.8/10,000 of hospital admissions [14, 15]. If we look at different regions of the world more closely, estimated prevalence is at 20.1% in Saudi Arabia, 1–5% in Asia, 5–9% in Europe, and 12–13% in Canada and North America [16]. White men who are in their fourth and fifth decade are affected most commonly [17]. A majority of the patients are present with acute, severe flank pain when a kidney

stone becomes impacted in the ureter due to obstruction, dysuria, strangury, and hematuria. Almost 70% of kidney stones are composed of calcium, and patients with calcium stones are more prone to further stone formation within 7 years [16].

Multiple predisposing factors have been identified for nephrolithiasis including metabolic diseases such as cystinuria (autosomal recessive) and hyperoxaluria, inherited conditions (polycystic kidney disease, renal tubular acidosis, hyperparathyroidism, and hypercalciuria), medications (triamterene, sulfonamides, carbonic anhydrase inhibitors, indinavir, acetazolamide, and corticosteroids), low urine volume, hypercalciuria (hyperparathyroidism and sarcoidosis), and hypocitraturia (distal renal tubular acidosis). Obesity is also associated with an increased risk of kidney stones, especially in women with a BMI over 40 [16].

Calcium oxalate stones constitute the majority (60%) of all renal stones, followed by calcium phosphate types (hydroxyapatite 20% and brushite 2%) and struvite stones (7–13%) usually composed of calcium-magnesium-ammonium phosphate. Struvite stones are formed secondary to urease positive bacterial infection and the most common composition of staghorn calculi. If struvite stones do not contain calcium like cystine stones, they become radiolucent and they are missed in radiographs.

Another radiolucent stone is uric acid stone with varying prevalence from 40% in Israel to 10% in the USA [16]. Hyperuricosuria, acidic urine, and low urinary volume are predisposing factors for urate stone. Radiolucent stones can be detected with ultrasound as well as calcium stones.

The main aims of imaging in patients with nephrolithiasis are to assess the size, number, and location of the stone(s), to reveal if there are complications, and to evaluate the contralateral kidney. Ultrasound can be applied to show dilatation of the collecting system, to identify stones, to assess the renal size and renal cortical thickness, and to detect complications. Hydration is very important before the examination, which increases the sensitivity from 24–73% to 85–100%, and increases the specificity from 74 to 83–100% [16, 18].

The composition of the stone does not affect the diagnostic sensitivity and specificity of ultrasound, while the calculus size and position and the body habitus may affect the detection rate along with the experience of the examiner.

The typical appearance of kidney stones is hyperechoic foci with acoustic shadowing (**Figure 3**). Kidney stones need to be at least 4–5 mm to be identified conspicuously on ultrasound [16]. For better visualization, the most appropriate transducer frequency tissue should be considered with a balance of tissue penetration and resolution. The focal zone should be adjusted at the level of stone for maximized shadowing. Furthermore, the detection of kidney stones and the visibility of posterior shadowing are significantly improved by tissue harmonic imaging [19]. Concomitant ultrasound findings in a patient with inflammation due to renal colic are increased echogenicity of renal parenchyma, dilatation of the collecting system, and subcapsular collections (urinomas). The application of color Doppler ultrasound which reveals twinkling artifact posteriorly in 83% of kidney stones improves the detection of small calculi [20].

Several mimickers for kidney stones at ultrasound may result in false-positive diagnosis, including intrarenal gas, renal artery calcification, calcified sloughed papilla, calcified transitional cell tumor, alkaline-encrusted pyelitis, and encrusted ureteral stents.

Nephrocalcinosis is a condition that is caused by hypercalcemia and hypercalciuria due to various diseases. Histologically, tissue calcification can be classified into two groups: calcification in normal and abnormal tissue. Dystrophic calcification arises in abnormal tissues such as vessels, haematoma, tumors, and inflammatory masses and when the solubility of the product of calcium and phosphate is exceeded due to pH changes or a reparative process. This is not considered to be

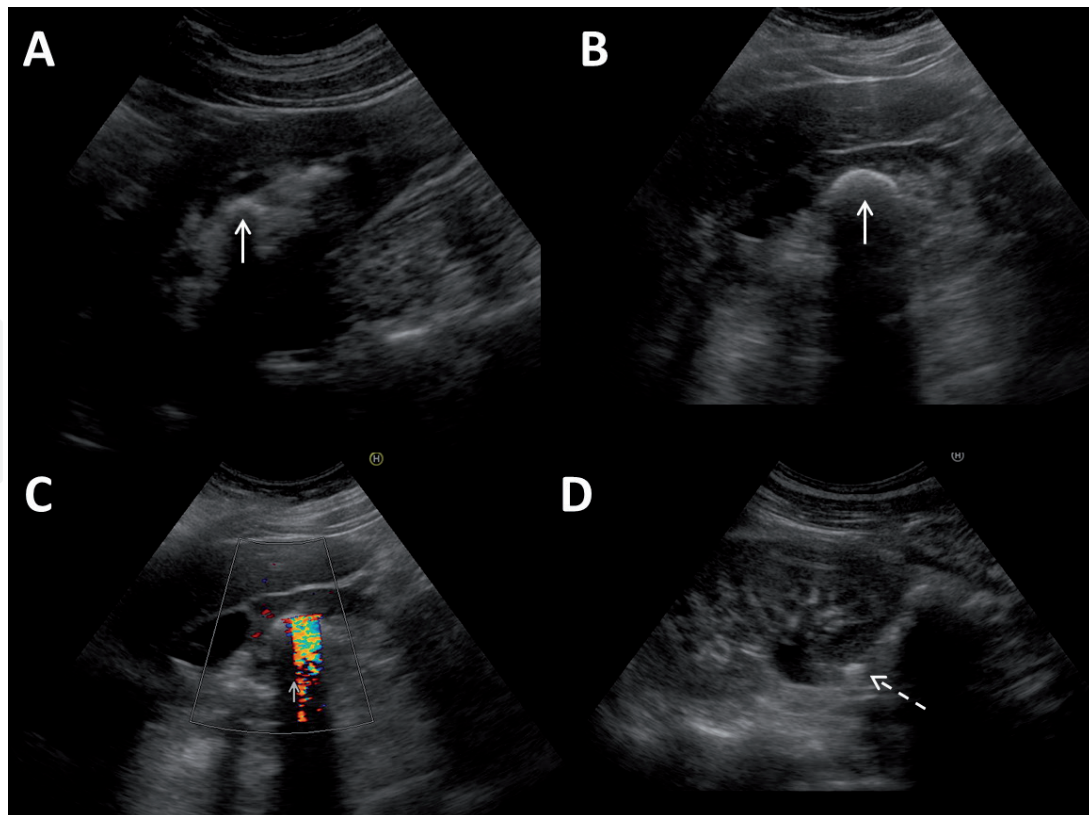


Figure 3.
Examples of kidney stone (arrow) in image (A–C) as a hyperechoic lesion with acoustic shadowing. In image (D), proximal ureteric stone (dashed arrow) and collecting system dilatation due to obstruction are demonstrated.

nephrocalcinosis. On the other hand, metastatic calcification occurs in normal tissues such as kidneys. It is usually due to abnormal biochemistry, that is, elevated serum calcium. The metabolic imbalance results in metastatic calcification when the solubility of calcium and phosphate or oxalates in extracellular fluid is exceeded.

Metastatic calcification in kidney is further subdivided anatomically into medullary nephrocalcinosis or cortical nephrocalcinosis. Medullary nephrocalcinosis accounts for the 97.6% of nephrocalcinosis and common causes are hyperparathyroidism, renal tubular acidosis, medullary sponge kidney, bone metastases, chronic pyelonephritis, Cushing's syndrome, hyperthyroidism, malignancy, renal papillary necrosis, sarcoidosis, sickle cell disease, hypervitaminosis D, and Wilson's disease. Cortical nephrocalcinosis constitutes the remaining 2.4%, and the common etiologies are acute cortical necrosis, ethylene glycol poisoning, chronic glomerulonephritis, chronic hypercalcemic states, sickle cell disease, and rejected renal transplants [21].

Cortical nephrocalcinosis is seen outlining of the kidney and along the columns of Bertin. It is usually due to severe destructive cortical disease, often observed in patients with end-stage renal failure. Any form of chronic glomerulonephritis may result in cortical nephrocalcinosis. Acute cortical necrosis often related to course of hypovolemic shock and eclampsia may give rise to patchy calcification in the renal parenchyma [16]. Ultrasonographic features of cortical nephrocalcinosis are increased cortical echogenicity representing early cortical calcification. Further progressive calcification may result in hyperechoic rim with extensive shadowing.

Medullary nephrocalcinosis is characterized by diffuse calcium deposition within the renal pyramids. Normally, calcium is removed by lymphatics in renal medulla, and if the amount of calcium exceeds lymphatic capacity, calcium deposits in the fornical tip and margins of the medulla. The typical ultrasound features of early medullary nephrocalcinosis may be nonshadowing echogenic rims surrounding medullary pyramids (**Figure 4**). As the disease progresses, hyperechogenicity fills the entire

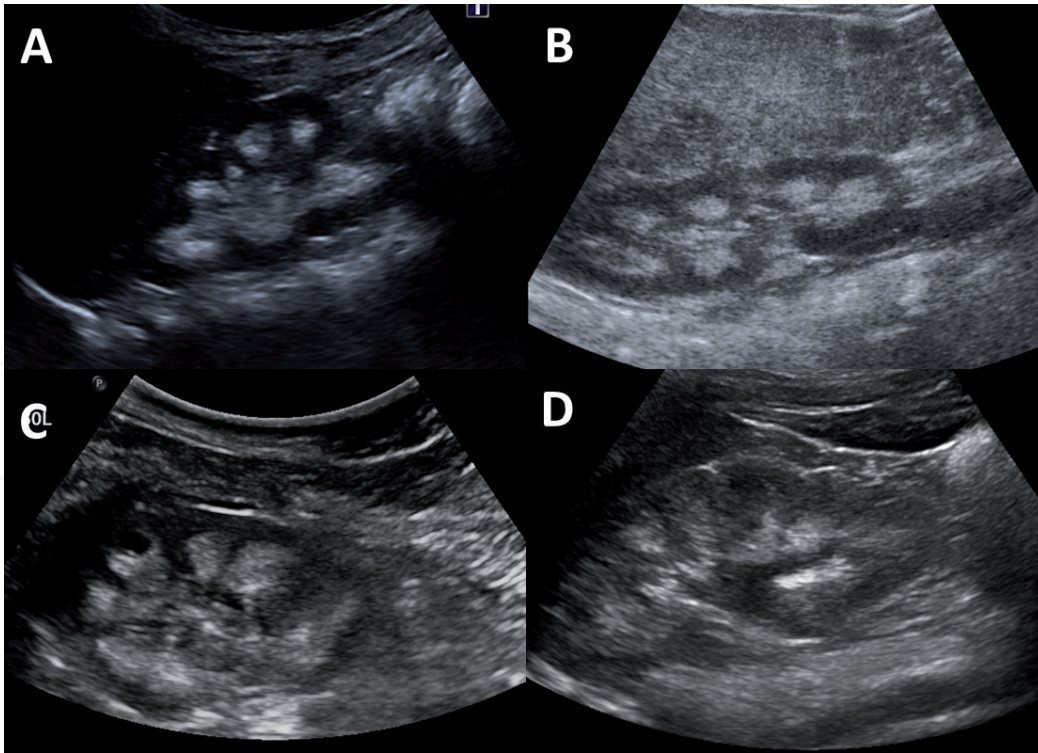


Figure 4.
Four patients with medullary nephrocalcinosis due to different etiology, such as hyperparathyroidism (A), Wilson's disease (B), and medullary sponge kidney (C and D). In all patients, the calyceal system is seen hyperechogenic.

pyramids. However, increased medullary echogenicity may also be seen in medullary sponge kidney; even it may be a physiologic transient finding in neonates [22]. In a similar way to cortical nephrocalcinosis, further calcium deposition induces acoustic shadowing at ultrasound in medullary nephrocalcinosis. These firm calcifications may perforate the caliceal wall and compose a nidus for further stone formation.

6. Cystic disease of kidney

Renal cystic disease is an entity that includes an enormous range of disorders including developmental (simple and complex cysts, localized cystic diseases, extraparenchymal sinus cysts, medullary sponge kidney, and multicystic dysplastic kidney), acquired (acquired cystic kidney disease), and hereditary (autosomal dominant polycystic kidney disease, autosomal recessive polycystic kidney disease, tuberous sclerosis complex, and von Hippel–Lindau disease) origin. Ultrasound is the primary and the most commonly used imaging modality for cystic renal disease but insufficient for the exact diagnosis in most of the cases. Key imaging features are the location, distribution, size, and composition of renal cysts as well as other coexisting noncystic renal lesions for the diagnosis [23].

Simple renal cysts are benign, fluid filled homogenous, and asymptomatic lesions, most of which are incidentally discovered on ultrasound. Prevalence of simple cysts increases with age in up to 27% of patients greater than 50 years of age [24]. They can be single or multiple, unilateral or bilateral, and commonly located in the renal cortex. Simple cysts are typically anechoic, round, or ovoid, with acoustic enhancement and no prominent wall thickness (**Figure 5**). If all these features are met with ultrasound, further evaluation or follow-up of the cyst is not required. All other sonographic findings, such as internal echo, septum, wall thickening, calcification, or acoustic shadowing, lead to the diagnosis of complex cyst.

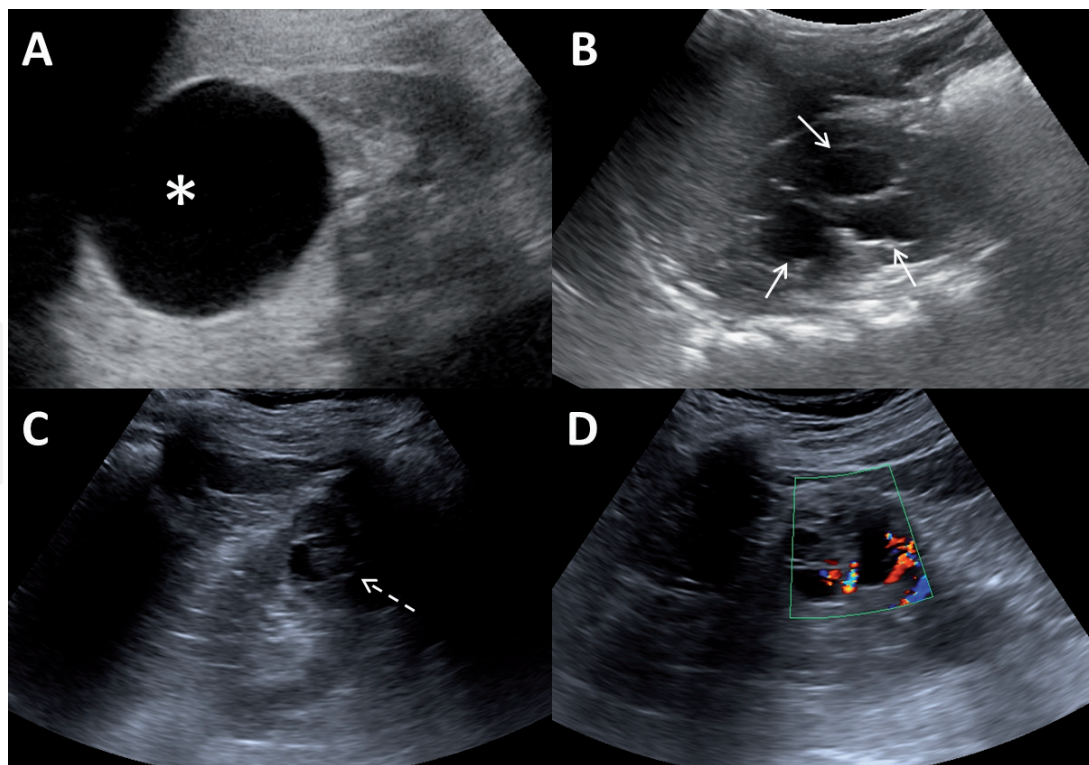


Figure 5. Simple cyst of the kidney (asterix) should be purely anechoic with no septations and solid component (A). Also increased through transmission can be seen posteriorly. Hydronephrosis (B) is seen as a multiple cystic structure (arrows) which is actually dilated calyx. In image (C), cystic lesion with multiple irregular septations is demonstrated (dashed arrow). On color Doppler ultrasound (D), vascularity in the septations is shown. Histopathologic evaluation confirmed the diagnosis of this cystic lesion as a clear cell type renal cell carcinoma.

Internal echoes within a cyst are generally due to hemorrhage or infection as in septations. Calcification can be seen in cyst wall or septa and may be fine and linear or amorphous and thick according to the shape. Thin wall or septal calcification suggests a complicated cyst rather than malignancy, while thick, irregular, amorphous calcification, perceptible, thickened walls, or mural nodularity should raise suspicion for malignancy, and further contrast enhanced imaging should be done (Figure 5C,D). Layering milk of calcium is seen as an echogenic focus with ring-down artifact in septa or cyst wall suggest that the cyst has a benign nature [25].

The most widely used classification system for complex renal cysts was introduced in 1991 by Bosniak [26], who grouped renal cysts into five categories based on imaging appearance in an attempt to predict the risk of malignancy and determine the outcome and management of complex cysts and cystic neoplasm (Table 1).

Extraparenchymal cysts are commonly seen in renal sinus and subdivided into parapelvic cyst and peripelvic cyst. Parapelvic cysts originate from the renal parenchyma and extend into the renal sinus, while peripelvic cysts arise directly in the renal sinus presumably due to lymphatic obstruction. Although these cysts differ in their origin, they are indistinguishable sonographically and benign nature, without a need for further imaging and follow up. However, these cysts may mimic hydronephrosis. Shape and extension of the cyst and concomitant caliceal dilatation of hydronephrosis are useful findings for differentiation [23].

Medullary cystic disease and juvenile nephronophthisis have similar imaging findings that are both composed of small multiple cysts at the corticomedullary junction and medulla. Juvenile nephronophthisis is an autosomal recessive condition usually present in childhood and generally progresses to end stage renal disease. On the other hand, medullary cystic disease is an autosomal dominant disorder present in the third or fourth decade of life with similar renal symptoms.

Autosomal dominant polycystic kidney disease (ADPKD) is the most common inherited renal disorder that is characterized by the progressive development of multiple asymmetrical and different sized cysts and marked renal enlargement [28]. ADPKD accounts for 10–15% of patients receiving dialysis and is the fourth leading cause of end stage renal disease in the world [23, 25]. Ultrasound is commonly used as a screening tool for the children of affected individuals (**Figure 6A**). According to Pei et al. [29], when evaluating patients with a positive family history of ADPKD, the number of renal cysts required for diagnosis is at least three (unilateral or bilateral) in subjects between 15 and 39 years old, at least two in each kidney in subjects between 40 and 59 years old, and at least four in each kidney in subjects more than 60 years old. Most of the cysts are simple cysts with varying size, which may be complicated by hemorrhage or infection and have thick walls, internal echoes, and/or fluid debris levels. Calcification in the cyst wall or stones may be seen as echogenic foci with acoustic shadowing. Most common associated extrarenal cysts of ADPKD are seen in liver, followed by pancreas, spleen, epididymis, seminal vesicle, uterus, ovary and thyroid [23]. Cerebral berry aneurysms, abdominal aortic aneurysm, cardiac valve diseases, and colonic diverticula may also accompany [25].

Autosomal recessive polycystic kidney disease (ARPKD) is characterized by renal tubular ectasia (manifesting as multiple bilateral renal cysts) and hepatic ductal plate malformation (leading to hepatic fibrosis and Caroli's disease) [23]. It is divided into four types depending on the age of onset: antenatal, neonatal, infantile, and juvenile forms. In the earlier age group, the more severe renal findings and the less pronounced hepatic involvement are encountered [30]. Ultrasound features of renal-dominant ARPKD include a lack of corticomedullary differentiation and massively enlarged, echogenic kidneys (**Figure 6B**). The increased echogenicity is due to the unresolved 1–2 mm cystic dilatation of the collecting tubules, which increases the number of acoustic interfaces. In neonates, small cysts may be revealed more clearly with high frequency linear-arrayed transducers.

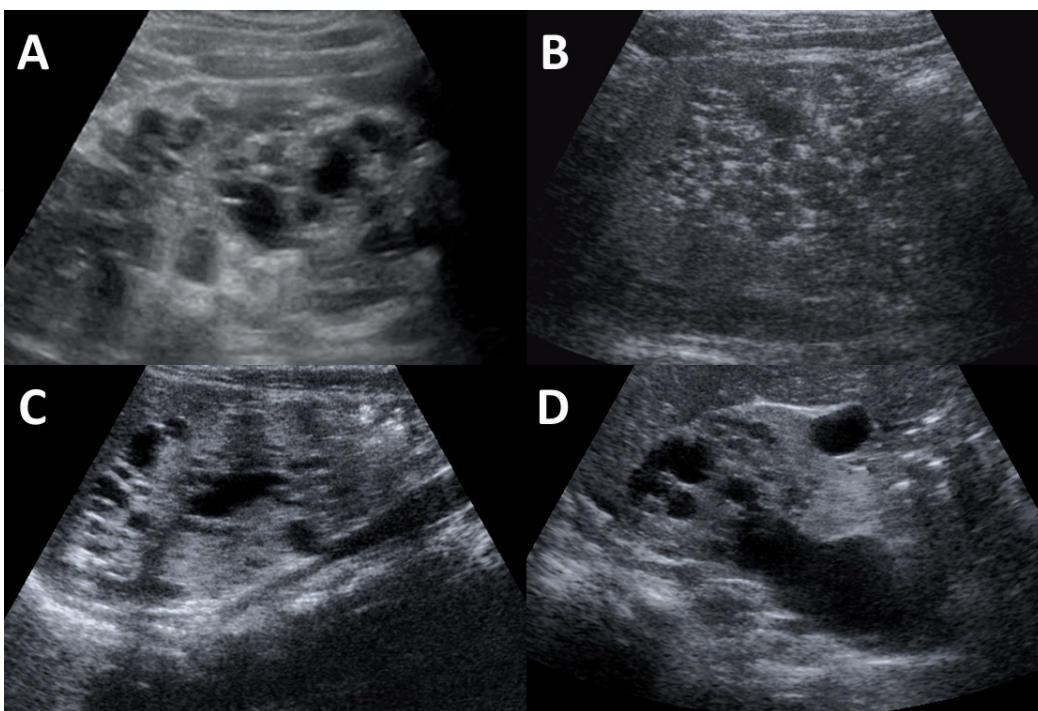


Figure 6. Ultrasound images of different renal cystic diseases, autosomal dominant polycystic kidney disease (A), autosomal recessive polycystic kidney disease (B), acquired cysts after chronic dialysis with end stage renal disease (C), and cystic renal dysplasia of newborn (D).

Localized cystic disease is a rare, benign condition that may mimic ADPKD. It is characterized by a cluster of simple cysts localized in either a portion of kidney (segmental cystic disease of the kidney) or an entire kidney (unilateral cystic disease of the kidney) [31]. On ultrasound, it appears as a conglomerate mass of multiple cysts of varying size separated by normal or atrophic kidney parenchyma. Lack of cysts in the contralateral kidney and other organs differentiates the disease from ADPKD [25].

Acquired cystic kidney disease (ACKD) is a progressive disorder, which occurs in the native kidneys of patients with end stage renal disease undergoing either chronic hemodialysis or peritoneal dialysis (**Figure 6C**). The prevalence of ACKD depends on the duration of dialysis and accounts for 40–60% of patients by 5 years and over 90% by 10 years of dialysis. Although the affected kidneys are usually atrophic at the time of cyst development, they may have an enlarged appearance due to the formation of extensive renal cysts and thus resemble ADPKD in some cases [32]. Three to five cysts in each kidney at ultrasound and increase in number in follow-up in a patient with chronic dialysis are diagnostics for ACKD [25].

Multicystic dysplastic kidney (MCDK) is a nonhereditary, developmental disorder characterized by multiple renal cysts replacing functional kidney parenchyma in the affected entire or segmented kidney which is smaller and has a distorted appearance. It is the most common cystic disease in pediatric population with an incidence of 1:4000. The exact etiology is unclear but proposed underlying causes are genetic disturbances, teratogens, in utero infections, and more commonly urinary tract outflow obstruction [33]. Ipsilateral renal anomalies, such as vesicoureteral reflux, or contralateral renal anomalies such as ureteropelvic junction obstruction are usually associated with MCDK. Typical sonographic findings include multiple cysts without communication, absence of normal parenchyma, and renal sinus among the cysts. Focal hyperechoic areas representing primitive mesenchyma or tiny cysts can be seen between the cysts [25]. Since many of the MDCKs involute over time, follow-up with ultrasound is recommended and nephrectomy should be reserved for the cases with hypertension, malignant transformation, or exceptionally large cystic kidneys [34].

Cystic renal dysplasia is the consequence of a developmental anomaly composed of abnormal structural organization and development of metanephric elements (**Figure 6D**). Both kidneys are affected and may have multiple cysts. It is often associated with urinary tract obstruction and may be seen with posterior urethral valve, prune belly syndrome, and ureteropelvic junction obstruction. This suggests that obstruction and urinary retention may cause anomalous kidney development [35].

Multilocular cystic nephroma (MLCN) is a rare benign disorder, composed of multiple noncommunicating cysts contained within a well-defined capsule and occasionally affects both kidneys. It has a trimodal age distribution that is seen in male patients less than 4 years of age and in female patients aged 4–20 or 40–60 years. MLCN is generally asymptomatic or may present with abdominal pain, hematuria, and hypertension. If the cysts of MLCN are tiny, a more solid-appearing echogenic mass will be present that precludes to differentiate MLCN from cystic RCC with ultrasound [25].

Chronic lithium nephropathy (CLN) is caused by long-term treatment with lithium salts that result in chronic tubulointerstitial nephropathy. In up to 62% of cases with CLN, typical findings of multiple small cysts (<2 mm) localized in both the cortex and the medulla uniformly and symmetrically distributed are observed [36]. Due to small size, cysts may not be recognized with ultrasound in some patients and magnetic resonance imaging is required for delineation.

7. Solid kidney lesions

Angiomyolipoma (AML) is the most frequent mesenchymal benign neoplasms of the kidney with a prevalence of 0.3–3% and with a female preponderance [37]. It is composed of varying amounts of adipose tissue, smooth muscle cells, and blood vessels [25]. It is frequently associated with an autosomal dominant phakomatosis syndrome, and with lymphangioliomyomatosis, a progressive disease which usually affects the lungs of young women and which is also related to tuberous sclerosis. In up to 80% children with tuberous sclerosis, AMLs are usually seen as bilateral, small, and multifocal. However, in sporadic patients, AMLs are typically unilateral and discovered in middle-aged women.

Small AMLs typically appear as homogenous hyperechoic lesion, sharply margined with detectable shadowing (**Figure 7**). Since larger AMLs may be more heterogeneous, it may be difficult to differentiate them from RCC and retroperitoneal liposarcoma. Magnetic resonance imaging should be indicated for these lesions. AMLs may rarely behave locally aggressive, with infiltration to the adjacent lymph nodes or within the inferior vena cava. Small, asymptomatic AMLs may be followed but if they are larger than 3–4 cm, they may be complicated by hemorrhage, which can be spontaneous or associated with relatively minor or incidental trauma. Bleeding may occur either within the tumor, or in the adjacent renal parenchyma, subcapsular, or retroperitoneal area. Complicated AMLs are treated surgically or by selective embolization [38].

Due to the lack of lymphoid tissue in the normal kidney, lymphomatous involvement of the kidney occurs from either hematogenous dissemination or from infiltration of retroperitoneal disease [25]. The kidneys are the 6th most affected abdominal organ after spleen, liver, gastrointestinal tract, pancreas, and abdominal wall [39]. Renal involvement is usually bilateral and found in one third of lymphoma patients at autopsy series [25]. Five different ultrasound appearances are recognized for renal lymphoma, depending partially on the growth pattern of the tumor: (1) single mass, (2) multiple masses, (3) infiltrative disease, (4) perirenal disease, and (5) invasion from retroperitoneal disease [40]. Focal masses appear as hypoechoic or anechoic homogenous lesions. If they are anechoic, they can be differentiated from cysts with the absence of increased through-transmission behind the lesion [25]. Diffuse infiltration may usually enlarge the kidney and decrease echogenicity despite disruption of renal architecture. Isolated perirenal involvement is very rare (<10% of cases of perirenal lymphoma) and appears as a soft tissue mass involving the perirenal space partially or completely and compresses but does not infiltrate the kidney [40]. Perirenal disease is frequently a part of retroperitoneal extension. Perirenal or retroperitoneal tumor may be confused with hematoma or extramedullary hematopoiesis. The lack of renal venous invasion, despite extensive retroperitoneal and renal sinus invasion, may help in differentiating renal lymphoma from renal cell carcinoma (RCC). Contrast-enhanced CT and MRI are superior to ultrasound for diagnosis of renal lymphoma (higher sensitivity and specificity) and in evaluating the extent of disease [40].

Leukemia involves the kidney either diffusely or with focal masses. Leukemic infiltration of the kidney has been reported in 65% of patients at autopsy series [25]. Although the typical ultrasound appearance of renal leukemia is bilateral kidney enlargement, in 15% of the leukemia patients, the kidney may enlarge without leukemic infiltration [25]. Renal leukemia may also be manifested as single or multiple focal masses or a coarsened parenchymal echo pattern with a distorted central sinus echo complex. These patients are more prone to renal, subcapsular, perirenal, or retroperitoneal bleeding.

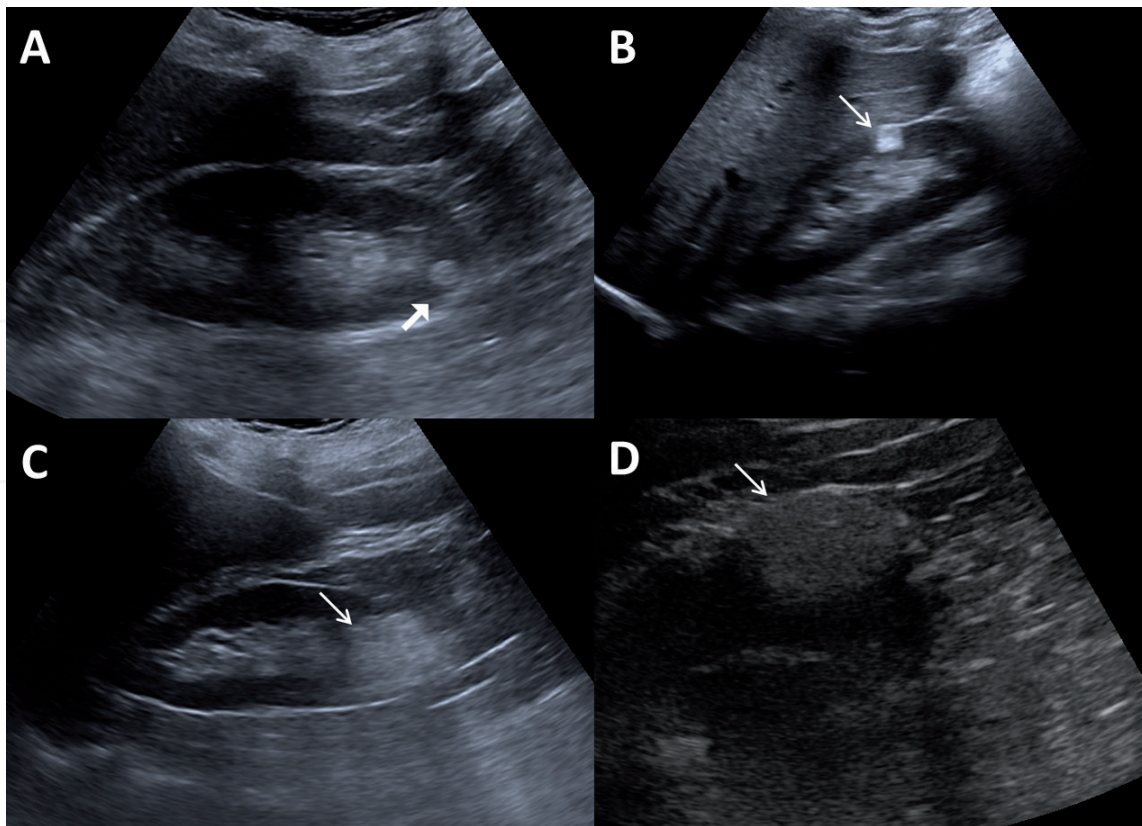


Figure 7.
Different patients with angiomyolipoma (arrows) with different sizes (A, B, C, D). Although appearances of the lesions are different, they are typically hyperechoic.

Renal cell carcinoma (RCC) is the most common primary kidney malignancy in adults and constitutes 86% of all primary malignant renal tumors and 3% of all adult malignancies [25]. RCC most often occurs in patients aged 50–70 years with 2:1 male predominance [41]. Most of the RCCs appear solid on ultrasound without any specific echogenicity. Smaller RCCs are more hyperechoic and can be misdiagnosed as AML at ultrasound. Several distinguishing characteristics are hypoechoic rim or cystic spaces more common in RCCs, while weak posterior acoustic shadowing can be seen more often in AMLs [25].

The most common subtype of RCC is clear cell (70–75%), followed by papillary (15%), chromophobe (5%), and oncocytic (2–3%) subtypes [25]. The last three have much better prognosis than clear cell RCC. Although ultrasound is much less accurate than CT or MRI for characterization of tumor content, lack of cystic necrotic areas and the presence of calcification, which are more common in papillary and chromophobe subtypes, appear to be associated with a better prognosis. Ultrasound may also demonstrate additional findings related to RCCs, including hydronephrosis; vascular encasement with diminished Doppler flow to the area of involvement or deterioration of the normal central sinus echo complex may be seen [41].

Cystic RCCs account for 5–7% of all RCCs. Four subtypes have been described for cystic RCCs at ultrasound: (1) unilocular, (2) multilocular, (3) necrotic (cystic necrosis), and (4) tumors emerging in a simple cyst. Since the unilocular and multilocular subtypes behave less aggressive, recognition of subtypes may have clinical importance [25]. The typical sonographic features of a unilocular RCC are a debris-filled mass with thick, irregular capsule that may have calcifications. Multilocular RCC may manifest as a cystic mass with internal septations which are thick (>2 mm) and nodular and may contain calcification. Necrotic RCCs have varying appearance depending on the degree of tumor necrosis. RCCs originating

in a simple cyst are very rare and usually seen in Von Hippel Lindau disease patients. A solid mural nodule can be seen at the base of a simple cyst at ultrasound.

Transitional cell carcinoma (TCC) of the renal pelvis is the second most common primary kidney tumor with a prevalence of 7%, but it is 50 times less common than bladder TCCs. Renal TCCs are typically seen in elderly men who are admitted with gross or microscopic hematuria in 75% and flank pain in 25%. The variable appearance of renal sinus beclouds the evaluation of renal pelvis TCCs. Patients at increased risk for development of TCC (such as patients with Balkan nephritis, vesicoureteral reflux, analgesic abuse, heavy smoking habit, exposure to carcinogens, or cyclophosphamide therapy) may require close follow-up. Papillary TCCs appear as solid, central, hypoechoic masses in renal with or without associated proximal calyceal dilatation. The differential diagnosis of these masses includes fibrin clots, sloughed papillae, and mycetoma [25].

Kidney metastases are usually seen on imaging for staging without any symptoms and have an incidence of 2–20% at autopsy series. Renal involvement is generally due to hematogenous spread. The most common primary tumor that metastasizes to kidney is lung carcinoma followed by breast carcinoma and RCC of the contralateral kidney [25]. Colon adenocarcinoma usually has solitary metastasis as a solid lesion on ultrasound which is indistinguishable from RCC [25]. Involvement of perirenal and retroperitoneal space is particularly seen in malignant melanoma and lung cancer metastasis [25]. Infiltrating metastases with subtle margins may be misdiagnosed with ultrasound and contrast enhanced imaging is required for further delineation.

8. Infections

Acute pyelonephritis is defined as an inflammation of the kidney and renal pelvis and has typical symptoms consisting of an abrupt onset of chills, high-grade fever ($>38.5^{\circ}\text{C}$), and unilateral or bilateral flank pain with costovertebral tenderness. Middle aged females are most commonly affected and *Escherichia coli* is by far the most common pathogen accounting for 80% of community-acquired and 50% of hospital-acquired infections most frequently due to ascending urinary tract infections [42]. In children, recurrent pyelonephritis commonly occurs as a result of vesicoureteral reflux.

The vast majority of acute pyelonephritis patients have normal findings on ultrasound. However, the following findings of pyelonephritis may be identified: kidney enlargement, abnormal echogenicity, loss of corticomedullary differentiation, ill-defined hyperechoic mass (es) (in focal pyelonephritis), compression of the renal sinus, and gas within kidney parenchyma (emphysematous pyelonephritis) (**Figure 8**). Untreated acute pyelonephritis may complicate with necrosis and abscess formation. Acute abscesses usually appear as a hypoechoic mass with increased through transmission posteriorly and indistinct margins. Over time, the abscess wall will be thickened and fluid levels will be developed within the abscess cavity [42]. Emphysematous pyelonephritis (EPN) is a rare, life-threatening infection seen in diabetic patients characterized by gas formation in the renal parenchyma. Dirty shadowing is revealed on ultrasound in EPN and contrast enhanced CT should be preferred for imaging to determine the location and extent of renal and perinephric gas [25].

Fungal infections of the kidney usually affect patients with diabetes mellitus, chronic indwelling catheters, malignancy, chronic antibiotic or steroid therapy, transplantation, and IV drug abusers [43]. *Candida albicans* is the most common fungal agent involved in genitourinary infections. Fungal infections usually manifest as unilateral small parenchymal abscesses which are tiny, hypoechoic, cortical

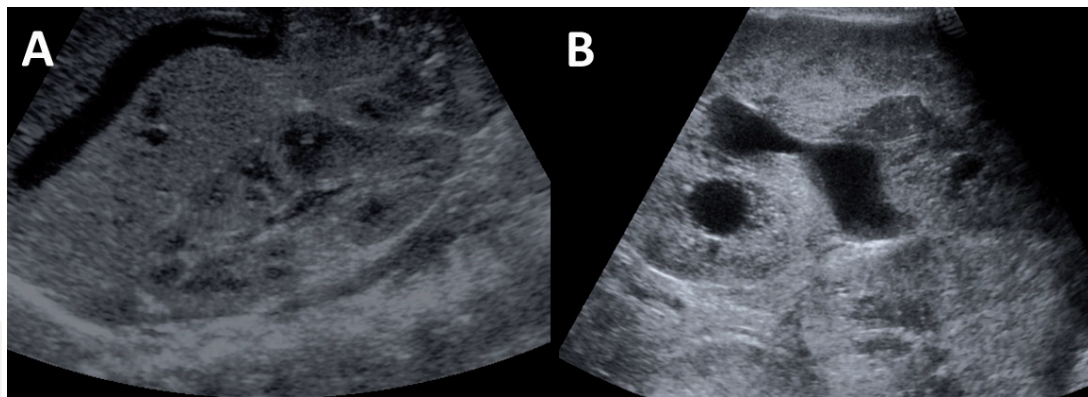


Figure 8. Two patients with acute pyelonephritis (A and B). Although the majority of the acute pyelonephritis has normal ultrasound appearance, in severe form of the disease, kidney enlargement and increased echogenicity of the kidney can be seen. In image (B), collecting duct dilatation is also seen which might be due to obstructive stone in the ureter.

lesions that may calcify over time [25]. Invasion of the collecting system results in fungus balls which are seen as hyperechoic soft tissue masses without posterior acoustic shadowing within the collecting system [43]. Fungus balls are motile and cause obstruction that may be associated with varying degrees of hydronephrosis on ultrasound.

9. Trauma

Renal injury occurs in 8–10% of patients suffering from blunt or penetrating trauma [44]. Blunt injury is far more common than penetrating injury accounting for 66–90% of cases and the majority of blunt trauma patients have relatively minor injuries which heal without any treatment. While blunt injuries are most often caused by motor vehicle accidents, falls, and direct impact from assault or sports competition, penetrating injuries are usually the result of gunshot or stab wounds. Patients with renal lesions (such as cysts, tumor, or hydronephrosis) are more prone to severe injury. The broadly accepted renal injury grading system constituted by the American Association for the Surgery of Trauma (AAST) is shown in **Table 1** [27].

Most patients with grade I and II injury are managed conservatively, while grades IV and V often require surgical treatment [27]. Contrast enhanced computed

AAST injury grading	Description
Grade I	Renal contusion or subcapsular hematoma with intact capsule
Grade II	Superficial cortex laceration (≤ 1 cm) that does not extend to deep medulla or the collecting system or nonexpanding hematoma
Grade III	Deep laceration(s) (>1 cm) with or without urine Extravasation
Grade IV	Laceration(s) extending into the collecting system with contained urine leak
Grade V	Shattered kidney, renal vascular pedicle injury, or devitalized kidney

Table 1. Renal injury grading scale of the American Association for the Surgery of Trauma [27].

tomography is the premier imaging modality for the evaluation of renal trauma. Technical limitations usually hinder an adequate examination with ultrasound in trauma patients. However, ultrasound may be used in the follow-up of patients with known kidney trauma [25]. Renal hematomas may be revealed as hypoechoic, hyperechoic, or heterogeneous depending on the stage of blood products. Lacerations are seen as linear hypoechoic defects that may extend through the kidney if a fracture is present and perinephric collections are associated with them. Subcapsular hemorrhage may appear as a perinephric heterogeneous fluid collection that flattens the underlying renal border. A shattered kidney in grade V trauma consists of multiple fragments of disorganized tissue with associated hemorrhage without normal renal architecture and urine collection in the renal bed.

10. Conclusion

Typical US features of the normal kidney and normal anatomic variants are very important to prevent over diagnosis and to recognize pathologic lesions. Moreover, typical US findings of benign lesions are extremely important to prevent unnecessary additional imaging and interventions. Although US is the first-line imaging and the second-line cross-sectional imaging modalities (CT and MRI) are performed in malignant disorders, radiologists and clinicians should be familiar with typical US appearances to narrow down differential diagnosis, to guide for most appropriate second-line imaging and for comprehensive follow-up.

Acknowledgements

The images are obtained from the archives of Istanbul Medeniyet University and Bingol State Hospital radiology archives.

Conflict of interest


The author declares no conflict of interest about this chapter.

Author details

Ercan Ayaz
Department of Radiology, Hacettepe University School of Medicine, Ankara,
Turkey

*Address all correspondence to: ercan.ayaz1@gmail.com

IntechOpen

© 2019 The Author(s). Licensee IntechOpen. This chapter is distributed under the terms of the Creative Commons Attribution License (<http://creativecommons.org/licenses/by/3.0>), which permits unrestricted use, distribution, and reproduction in any medium, provided the original work is properly cited. 

References

- [1] Zweyer M. Embryology of the kidney. In: Quaia E, editor. *Radiological Imaging of the Kidney*. Medical Radiology. Berlin, Heidelberg: Springer; 2010. pp. 3-16
- [2] Moore KL, Dalley AF, Agur AMR. *Clinically Oriented Anatomy*. 6th ed. Philadelphia: Wolters Kluwer/Lippincott Williams & Wilkins; 2010
- [3] Quaia E, Martingano P, Cavallaro M, Zappetti R. Normal radiological anatomy and anatomical variants of the kidney. In: Quaia E, editor. *Radiological Imaging of the Kidney*. Medical Radiology. Berlin, Heidelberg: Springer; 2014. pp. 17-74
- [4] Emamian SA, Nielsen MB, Pedersen JF, Ytte L. Kidney dimensions at sonography: Correlation with age, sex, and habitus in 665 adult volunteers. *American Journal of Roentgenology*. 1993;**160**:83-86
- [5] Netter FH. Anatomy, structure, and embryology. In: Shapter RK, Yonkman FF, editors. *The CIBA Collection of Medical Illustrations, Vol. 6. Kidneys, Ureters, and Urinary Bladder*. Summit, NJ, USA: CIBA Pharmaceutical; 1973. pp. 2-35
- [6] Friedenbergrm RM, Dunbar JS. Excretory urography. In: Pollack HM, editor. *Clinical Urography*. Philadelphia: Saunders; 1990. pp. 101-243
- [7] Platt JF, Rubin JM, Bowerman RA, Marn CS. The inability to detect kidney disease on the basis of echogenicity. *American Journal of Roentgenology*. 1988;**151**:317-319
- [8] Kasap B, Soylu A, Türkmen M, et al. Relationship of increased renal cortical echogenicity with clinical and laboratory findings in pediatric renal disease. *Journal of Clinical Ultrasound*. 2006;**34**:339-342
- [9] Yeh HC, Halton KP, Shapiro RS, et al. Junctional parenchyma: Revised definition of hypertrophic column of Bertin. *Radiology*. 1992;**185**:725-732
- [10] Leekam RN, Matzinger MA, Brunelle M, et al. The sonography of renal columnar hypertrophy. *Journal of Clinical Ultrasound*. 1983;**11**:491-494
- [11] Quaia E. Ultrasound of the kidney. In: Quaia E, editor. *Radiological Imaging of the Kidney*. Medical Radiology. Berlin, Heidelberg: Springer; 2014. pp. 83-121
- [12] Friedland GW, Devries PA, Nino-Murcia M, et al. Congenital anomalies of the urinary tract. In: Pollack HM, editor. *Clinical Urography: An Atlas and Textbook of Urologic Imaging*. Philadelphia, USA: Saunders; 1990. pp. 559-787
- [13] Talner LB. Specific causes of obstruction. In: Pollack HM, editor. *Clinical Urography: An Atlas and Textbook of Urological Imaging*. Philadelphia: Saunders; 1990. pp. 1629-1751
- [14] Menon M, Resnick MI. Urinary lithiasis: Etiology, diagnosis, and medical management. In: Walsh PC, Retik AB, Darracott VE Jr, editors. *Campbell's Urology*. Philadelphia, USA: WB Saunders; 2002. pp. 3229-3305
- [15] Sandhu C, Anson KM, Patel U. Urinary tract stones—Part I: Role of radiological imaging in diagnosis and treatment planning. *Clinical Radiology*. 2003;**58**:415-421
- [16] Phillips S, Tudor GR. Nephrocalcinosis and nephrolithiasis. In: Quaia E, editor. *Radiological Imaging of the Kidney*. Medical Radiology. Berlin, Heidelberg: Springer; 2014. pp. 391-410
- [17] Freeman SJ, Sells S. Investigation of loin pain. *Imaging*. 2008;**20**:38-56

- [18] Fowler KA, Locken JA, Duchesne JH, et al. US for detecting renal calculi with nonenhanced CT as a reference standard. *Radiology*. 2002;**222**:109-113
- [19] Ozdemir H, Demir MK, Temizöz O, et al. Phase inversion harmonic imaging improves assessment of renal calculi: A comparison with fundamental gray-scale sonography. *Journal of Clinical Ultrasound*. 2008;**36**:16-19
- [20] Lee JY, Kim SH, Cho JY, Han D. Color and power Doppler twinkling artifacts from urinary stones: Clinical observations and phantom studies. *American Journal of Roentgenology*. 2001;**176**:1441-1445
- [21] Banner M. Nephrocalcinosis. In: Pollack HM, editor. *Clinical Urography: An Atlas and Textbook of Urological Imaging*. Philadelphia, USA: Saunders; 1990. pp. 1768-1775
- [22] Khoory BJ, Andreis IA, Vito L, Fanos V. Transient hyperechogenicity of the renal medullary pyramids: Incidence in the healthy term newborn. *American Journal of Perinatology*. 1999;**16**:463-468
- [23] Bae KT, Furlan A, Mileto A. Renal cystic disease. In: Quiaia E, editor. *Radiological Imaging of the Kidney*. Medical Radiology. Berlin, Heidelberg: Springer; 2014. pp. 305-334
- [24] Tada S, Yamagishi J, Kobayashi H, et al. The incidence of simple renal cyst by computed tomography. *Clinical Radiology*. 1983;**34**:437-439
- [25] Tublin M, Thurston W, Wilson SR. The kidney and urinary tract. In: Rumack CM, Wilson SR, Charboneu JW, Levine D, editors. *Diagnostic Ultrasound*. 4th ed. Philadelphia, PA, USA: Elsevier Mosby; 2011. pp. 317-391
- [26] Bosniak MA. The small (≤ 3.0 cm) renal parenchymal tumor: Detection, diagnosis, and controversies. *Radiology*. 1991;**179**:307-317
- [27] Kozar RA, Crandall M, Shanmuganathan K, Zarza BL, Coburn M, Cribari C, et al. Organ injury scaling 2018 update: Spleen, liver, and kidney. *The Journal of Trauma and Acute Care Surgery*. 2018;**85**:1119-1122
- [28] Harris PC, Bae KT, Rossetti S, et al. Cyst number but not the rate of cystic growth is associated with the mutated gene in autosomal dominant polycystic kidney disease. *Journal of the American Society of Nephrology*. 2006;**17**:3013-3019
- [29] Pei Y, Obaji J, Dupuis A, et al. Unified criteria for ultrasonographic diagnosis of ADPKD. *Journal of the American Society of Nephrology*. 2009;**20**:205-212
- [30] Turkbey B, Ocak I, Daryanani K, et al. Autosomal recessive polycystic kidney disease and congenital hepatic fibrosis (ARPKD/CHF). *Pediatric Radiology*. 2009;**39**:100-111
- [31] Slywotzky CM, Bosniak MA. Localized cystic disease of the kidney. *American Journal of Roentgenology*. 2001;**176**:843-849
- [32] Bakir AA, Hasnain M, Young S, et al. Dialysis-associated renal cystic disease resembling autosomal dominant polycystic kidney disease: A report of two cases. *American Journal of Nephrology*. 1999;**19**:519-522
- [33] Hains DS, Bates CM, Ingraham S, et al. Management and etiology of the unilateral multicystic dysplastic kidney: A review. *Pediatric Nephrology*. 2009;**24**:233-241
- [34] Vester U, Kranz B, Hoyer PF. The diagnostic value of ultrasound in cystic kidney diseases. *Pediatric Nephrology*. 2010;**25**:231-240
- [35] Shibata S, Nagata M. Pathogenesis of human renal dysplasia: An alternative scenario to the major theories. *Pediatrics International*. 2003;**45**:605-609

- [36] Roque A, Heredia V, Ramalho M, et al. MR findings of lithium related kidney disease: Preliminary observations in four patients. *Abdominal Imaging*. 2012;**37**:140-146
- [37] Quaia E. Benign solid renal tumors. In: Quaia E, editor. *Radiological Imaging of the Kidney*. Medical Radiology. Berlin, Heidelberg: Springer; 2014. pp. 501-535
- [38] Silverman SG, Israel GM, Herts BR, et al. Management of the incidental renal mass. *Radiology*. 2008;**249**:16-31
- [39] Lee WK, Lau EW, Duddalwar VA, et al. Abdominal manifestations of extranodal lymphoma: Spectrum of imaging findings. *American Journal of Roentgenology*. 2008;**191**:198-206
- [40] Rappaport A, Oyen RH. Renal lymphoma and renal sarcoma. In: Quaia E, editor. *Radiological Imaging of the Kidney*. Medical Radiology. Berlin, Heidelberg: Springer; 2014. pp. 631-643
- [41] Hayashi D, Guermazi A, Holalkere NS. Imaging in renal cell carcinoma. In: Quaia E, editor. *Radiological Imaging of the Kidney*. Medical Radiology. Berlin, Heidelberg: Springer; 2014. pp. 537-570
- [42] Blandino A, Mazziotti S, Minutoli F, Ascenti G, Gaeta M. Acute renal infections. In: Quaia E, editor. *Radiological Imaging of the Kidney*. Medical Radiology. Berlin, Heidelberg: Springer; 2014. pp. 411-436
- [43] Quaia E, Giarraputo L, Martingano P, Cavallaro M. Chronic renal infections and renal fungal infections. In: Quaia E, editor. *Radiological Imaging of the Kidney*. Medical Radiology. Berlin, Heidelberg: Springer; 2014. pp. 437-467
- [44] Mirvis SE. Imaging of renal trauma. In: Quaia E, editor. *Radiological Imaging of the Kidney*. Medical Radiology. Berlin, Heidelberg: Springer; 2014. pp. 483-498
- [45] Behrman RE, Kliegman RM, Arvin AM. *Nelson Textbook of Pediatrics*. 15th ed. Philadelphia: WB Saunders; 1996